International Journal of Multiphase Flow 36 (2010) 793–797

Contents lists available at ScienceDirect

International Journal of Multiphase Flow

journal homepage: www.elsevier.com/locate/ijmulflow

Recognition of gas–liquid two-phase flow patterns based on improved local binary pattern operator

Wenyin Zhang [a,*], Frank Y. Shih [b], Ningde Jin [c], Yinfeng Liu [a]

[a] School of Informatics, Linyi Normal University, Linyi, Shandong 276005, PR China
[b] College of Computing Sciences, New Jersey Institute of Technology, Newark, NJ 07102, USA
[c] School of Electrical Engineering and Automation, Tianjin University, Tianjin 300072, PR China

ARTICLE INFO

Article history:
Received 13 April 2010
Received in revised form 21 April 2010
Accepted 9 June 2010
Available online 15 June 2010

Keywords:
Local binary pattern
Two-phase flow regime
Support vector machine
Neural network

ABSTRACT

A new method to pattern recognition of gas–liquid two-phase flow regimes based on improved local binary pattern (LBP) operator is proposed in this paper. Five statistic features are computed using the texture pattern matrix obtained from the improved LBP. The support vector machine and back-propagation neural network are trained to flow pattern recognition of five typical gas–liquid flow regimes. Experimental results demonstrate that the proposed method has achieved better recognition accuracy rates than others. It can provide reliable reference for other indirect measurement used to analyze flow patterns by its physical objectivity.

1. Introduction

Nowadays, much more attention has been paid on the changing patterns and structures of multi-phase flows, which are extensively encountered in petroleum exploitation and transport, chemical engineering, nuclear reactors, and thermal systems. In the gas–liquid two-phase flow, the distribution of the two media, namely flow structure, is extremely complex and can vary instantaneously because of stochastic variation of gas–liquid two-phase flow interface. Therefore, it is crucial to understand the interior structure and flow properties of different flow patterns. At present, image and video processing technologies and high frame-rate photographic techniques are used to analyze the inner structure and flow properties of different flow patterns quantitatively and qualitatively. The aim is to develop a mathematical model and make a deep understanding of different temporal and spatial flow characteristics, as shown by Hsieh et al. (1997), Gopal and Jepson (1997), Shi et al. (2005), Sathyamurthi et al. (2007), Bui et al. (1999), Zhou et al. (2009).

As a matter of fact, many gas–liquid two-phase flow analysis and recognition methods based on image or video processing techniques have been developed in recent years. The dynamic images of two-phase flow patterns obtained by high frame-rate camera are characterized by direct-vision and physical objectivity, and are able to reflect the information about the complex two-phase flow structure to a certain extent. Hsieh et al. (1997) acquired dynamic images of gas–liquid two-phase flow in the riser in a natural circulation loop by CCD and gave the statistics about image gray-level distribution probabilities of four flow patterns, namely single-phase flow, bubbly flow, slug flow, and churn flow, to classify them and analyze their dynamic variations by image processing techniques. Gopal and Jepson (1997) studied the dynamic characteristics quantitatively, including local velocity and void distribution of slug flow in gas–liquid two-phase mixtures, by applying image processing techniques and the kinetics model of slug flow on the experimental conditions. Shi et al. (2005) presented image analysis to extract bubble features of gas–liquid two-phase flow images and employed the fuzzy inference algorithm to identify flow patterns. Sathyamurthi et al. (2007) applied high-speed dynamic photography and chaotic box-counting techniques to calculate fractal order of bubble voids in nucleate boiling wall, which consists of an array of individually controlled micro-heaters. Bui et al. (1999) presented a new method for automatic bubble identification of two-phase bubbly/slug flow. Recently, Zhou et al. (2009) used histogram to compute the flow image features and applied the support vector machine (SVM) to identify the flow patterns.

Although there are great progresses in studying the two-phase flow properties, most of the research schemes are based on single and standard image of typical flow pattern preprocessing to extract some characteristic parameters of flow patterns. In the two-phase flow process, the temporary flow patterns are various at different positions as a result of the stochastic variability of phase hold-up, flow structure, and the interfacial interaction. Therefore, it is

* Corresponding author.
E-mail address: zwy218@hotmail.com (W. Zhang).

0301-9322/$ - see front matter © 2010 Elsevier Ltd. All rights reserved.
doi:10.1016/j.ijmultiphaseflow.2010.06.002

worthy of studying on temporal and spatial evolution regularity of two-phase flow patterns using image processing techniques, and taking into account of flow pattern types and their dynamic development information.

In this paper, we first propose the improved local binary pattern (ILBP) operator to analyze the flow patterns and extract their flow texture properties. We then train the SVM and back-propagation (BP) neural network to identify the flow patterns. The original local binary pattern (LBP) operator is a typical texture analysis algorithm (see Maenpaa et al., 2000; Ojala et al., 2002; Ahonen et al., 2004, Maenpaa, 2003) and is widely used in the texture classification domain. However, it ignores the gray level variations of pixels in a neighborhood. We improve the LBP operator by considering the gray-level differences in texture description. In other words, we concentrate on the visually most important texture pattern parts of the images, without taking the unimportant details of the texture pattern into account. This allows gray level (or illumination) adaptability. Experimental results show that our method can extract the discriminate image features and obtain higher classification accuracies of the gas–liquid two-phase flow regimes, as compared with other approaches.

The remainder of this paper is organized as follows. In Section 2, we explain the method to capture gas–liquid two-phase flow videos with high-speed dynamic camera. In Section 3, we present the improved local binary pattern operator, and discuss how we improve the LBP operator to process the gas–liquid two-phase flow video for feature extraction. In Section 4, we describe the applications of SVM and BP neural network for flow pattern recognition. Finally, we conclude the paper in Section 5.

2. Information capture of gas–liquid two-phase flow images

The gas–liquid two-phase flow dynamic experiments in vertical upward pipes were carried out in the multi-phase flow loop at Tianjin University, China. The two-phase flow monitoring system consists of VMEA (see Sathyamurthi et al., 2007), a high-precision differential micro pressure sensor, a laser sensor, and a high-speed dynamic camera, called SpeedCam Visario (1536×1024, 1000 frames per second, 10 electronic shutters), based on CMOS technology produced by Weinberger Corporation. The parameters of the camera set in our experiment are as follows: resolution 640×480 and 200 frames per second. The measurement system is based on the virtual instrument technology with data acquisition board PXI 4472, which is manufactured by National Instrument Corporation. The sampling rate and recording time are respectively 400 Hz and 50 s. The tricolor fluorescent lamp with the color temperature 6500 K is acted as the illumining source, which is bright without glitter.

Owing to transparency of air and water, a black-lighted imaging technique (see Shi et al., 2005) is utilized to capture the shadow of bubble shape in different flow patterns. Because the flow pattern images will look nicer on the diffusion of backlighting, one or two pieces of the sulfated paper are pasted on outside of the pipe opposite the camera lens, so as to enhance quality of photographs.

The experimental media are air and tap water. The velocity of superficial water is from 0.02 m/s to 0.4 m/s, and the superficial gas velocity is from 0.005 m/s to 3.85 m/s. Five typical flow patterns in the vertical upwards pipe, namely, bubble flow, bubble–slug flow, slug flow, slug–churn flow, and churn flow, are shot as shown in Fig. 1. The images are affected by acrylic pipe cleanliness and the level of light, so some preprocessing procedures, such as anti-noise and image enhance, must be conducted to improve the image quality.

3. Local binary pattern based gas–liquid flow regime feature extraction

3.1. Local binary pattern

The local binary pattern (LBP) operator was proposed to measure the local contrast in texture analysis (see Maenpaa et al., 2000; Ojala et al., 2002). It has been successfully applied to visual inspection and image retrieval as shown by Maenpaa and Pietikainen (2003).

The LBP operator is defined in a circular local neighborhood. With the center pixel as the threshold, its circularly symmetric P neighbors within a certain radii R are labeled as 1 when its value is larger than the center or labeled as 0 when its value is smaller than the center. Note that $P = (2R + 1)^2 - 1$. Then, the LBP code of the center pixel is produced by multiplying the thresholded values (1 or 0) by weights given to the corresponding pixels, and summing up the result. For example, the LBP of a 3×3 window (where $R = 1$ and $P = 8$) uses the center pixel as a threshold value, and the values of the thresholded neighbors are multiplied by the binomial weight and summed to obtain the LBP number. In this way, the LBP can produce a number from 0 to 255. The entire LBP numbers composite a texture spectrum of an image with 256 gray levels. Given parameters P and R, which control the quantization of the angular space and spatial resolution respectively, the LBP number, denoted by LBP_p, is defined as

$$\mathrm{LBP}_P = \sum_{p=0}^{P-1} S(g_p - g_c) \times 2^p \tag{1}$$

where g_c denotes the gray level of the center pixel c in the P neighborhood, g_p denotes the gray level of the neighboring pixels p, and $S(x)$ refers to the sign function defined as

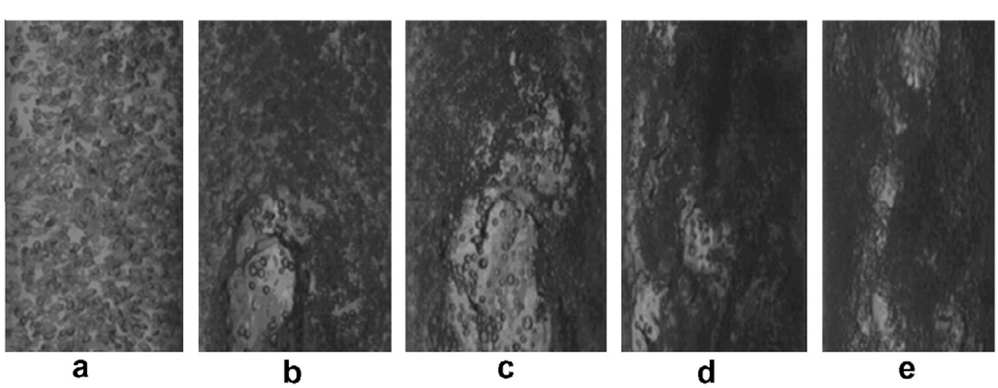

Fig. 1. Five typical flow patterns: (a) bubble flow, (b) bubble-slug flow, (c) slug flow, (d) slug-churn flow, and (e) churn flow.

$$S(x) = \begin{cases} 1, & \text{if } x \geqslant 0 \\ 0, & \text{otherwise} \end{cases} \tag{2}$$

More detailed information about LBP including its extensions, uniform, rotation invariance, and multi-scale can be referred to Ahonen et al. (2004) and Maenpaa (2003).

3.2. The improved LBP operator

The traditional LBP operator ignores the gray level changes of pixels and illumination adaptability. Therefore, we improve the LBP operator by considering the magnitude of gray-level differences, which is important in texture description. Our LBP operator concentrates on the visually most important texture pattern parts of images and disregards the unimportant details.

In the improved LBP operator, we introduce a parameter α to control the difference between neighboring pixels. If the difference between two pixels does not reach an extent controlled by α, we regard the two pixels as the same. The improved LBP operator is defined as

$$\mathrm{LBP}_P^{\alpha} = \sum_{p=0}^{P-1} S\left(\frac{g_p - g_c}{\bar{g}} - \alpha\right) \times 2^p \tag{3}$$

where $\bar{g}$ is the mean value of pixels in the neighborhood.

The improved LBP operator is based on the features of video frames captured by the two-phase flow monitoring system and ignores the non-significant details, so that it can extract the most important texture patterns. Fig. 2 shows the examples of applying the traditional LBP operator and the improved LBP operator. We can observe that the improved LBP operator can extract the main characteristic of the flow images.

3.3. Texture pattern matrix and its feature extraction

All the LBP numbers can composite a texture spectrum, named texture pattern matrix (TPM), which is a map of a flow image. The map can show the distribution of gray levels and the main texture information of the flow image. Five features can be extracted from the TPM. The first three features are average (denoted by AVE), deviation (DEV), and energy (ENE), and the other two statistics features are entropy (ENT) and correlation (COR).

Let $f(x, y)$ be the TPM of size $M \times N$. The five features are listed as follows:

$$\mathrm{AVE} = \frac{1}{MN}\sum_{x=0}^{M-1}\sum_{y=0}^{N-1} f(x,y) \tag{4}$$

$$\mathrm{DEV} = \sqrt{\frac{1}{MN}\sum\nolimits_{x=0}^{M-1}\sum\nolimits_{y=0}^{N-1}(f(x,y) - \mathrm{AVE})^2} \tag{5}$$

$$\mathrm{ENE} = \sqrt{\sum\nolimits_{x=0}^{M-1}\sum\nolimits_{y=0}^{N-1} f^2(x,y)} \tag{6}$$

$$\mathrm{ENT} = -\sum_{x=0}^{M-1}\sum_{y=0}^{N-1}\left(\frac{f(x,y)}{\mathrm{ENE}}\ln\left(\frac{f(x,y)}{\mathrm{ENE}}\right)\right) \tag{7}$$

$$\mathrm{COR} = \sum_{x=0}^{M-1}\sum_{y=0}^{N-1}\frac{xyf(x,y) - \mu_x\mu_y}{\sigma_x\sigma_y} \tag{8}$$

where μ is the mean value and σ is the standard deviation.

These five features were used to construct the dynamic images feature curves shown in previous work Zhang and Jin (2009). In this paper, we mainly focus on the flow pattern recognition. Fig. 3 shows five feature curves of five flow patterns in a 4-s high-speed flow video with parameters: $R = 1$, $P = 8$, and $\alpha = 0.15$.

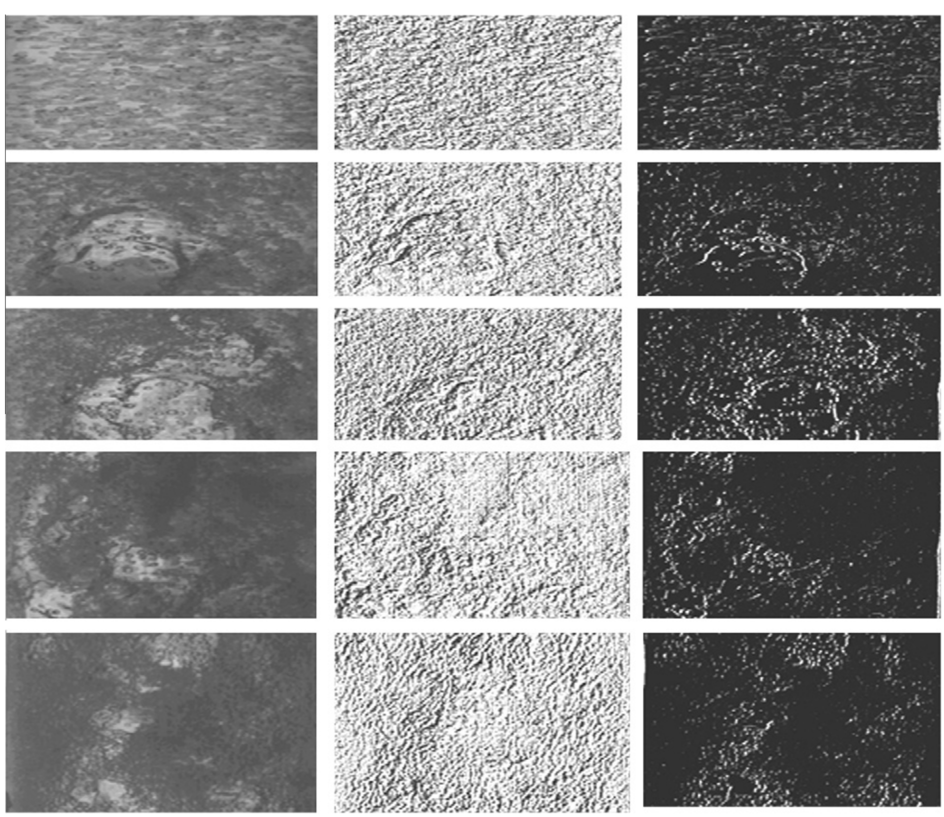

Fig. 2. Left column: the original flow images; middle column: results of the traditional LBP patterns ($R = 1$ and $P = 8$); right column: results of the improved LBP patterns ($R = 1$, $P = 8$, and $\alpha = 0.15$).

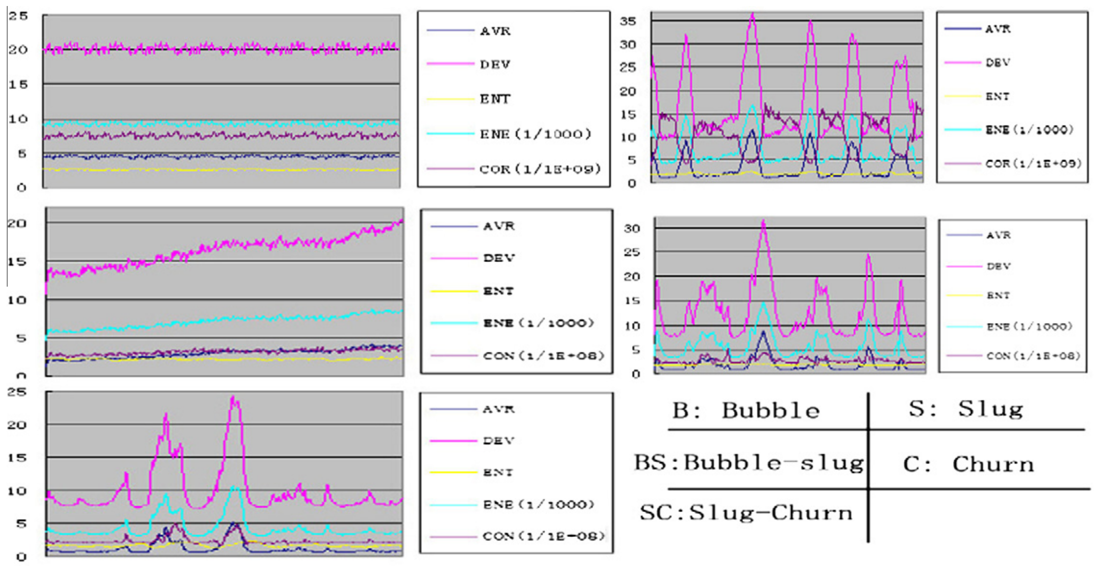

Fig. 3. Five feature curves of five flow patterns in a 4-second high-speed flow video with parameters: $R = 1$, $P = 8$, and $\alpha = 0.15$.

4. Pattern recognition of flow regimes

In this section, these features combined to establish the data set, and the support vector machine and BP neural network are used separately to realize the automatic recognition of the flow patterns.

4.1. Support vector machine

The support vector machine (SVM) was developed by Vapnik (1998) for pattern recognition and function regression. It has been proved to be successful in many other applications, including handwritten digit recognition, image classification, face detection, object detection, and text classification (see Cortes and Vapnik, 1995; Chang et al., 2000).

4.1.1. SVM parameters setting

We use the SVM implementation by libSVM tool, a C++ open source library constructed by Chang and Lin (2001) and Lin (2001) in our experiments. The SVM parameters are selected as follows:

- Type of SVM: We choose the type c-SVC.
- Kernel type: A radial basis function (RBF) kernel was used. Note that the RBF shows a better performance rate for classifying non-linear problems than other types of kernels.
- Example set: The example set is 2000 images extracted from video flow.
- Determination of parameter Gamma and cost *C*: The two parameters are decided by validating the classification accuracy of the testing examples. In the training process, cross-validation as shown in Lin (2001) was used. For every two parameter Gamma and *C*, we take the average classification accuracy as their corresponding accuracy. However, because of the large scope of Gamma and *C*, we used the parallel grid search algorithm as shown in Lin (2001) to find the Gamma and *C* with best accuracy. Here, we improve the search algorithm to save the searching time. Firstly, we search the best combination of Gamma and *C* in a large scope coarsely, and then we conduct the second search in a small scope based on the best combination. Finally, we obtain Gamma and *C* of SVM.

4.1.2. Experimental results by SVM

In the experiments, we divided the 2000 example image into odd and even parts. Odd part was normalized and used as the training set to train the SVM, and even part was used to test and validate the SVM. Experimental results show that the classification accuracy rates of testing examples and validating examples based on the improved LBP operator are 99.8% and 99.6% respectively, with an average of 99.7%; while using the traditional LBP operator, the average accuracy only reaches 94.1%. Table 1 shows the classification accuracies of the five flows using the SVM with the improved LBP (denoted by ILBP) as compared with the traditional LBP (denoted by TLBP). From the table, we can see that the recognition accuracies of bubble flow and bubble–slug flow reach 100%, and those of others are 99.5%. Churn flow and slug–churn flow can often be misclassified into slug flow. Because of the lacking discrimination of the traditional LBP operator, its result is about 5.9% lower than that of the improved LBP.

Zhou et al. (2009) used the SVM to identify the flow patterns of gas/water two-phase flows. They constructed the feature vector based on the image histogram, and obtained the classification accuracy of 99.04%. Zhao et al. (2006) also used the SVM to classify the flow patterns, but they extracted features in frequency domain by using the linear prediction method and in time domain by using the time series statistical analysis. The classification accuracy they

Table 1
Comparisons of classification accuracies of using SVM with ILBP and TLBP.

	Bubble	Slug	Bubble–slug	Churn	Slug–churn	Accuracies (%)	Method
Bubble	200	0	0	0	0	100	ILBP
	189	1	5	2	3	94.5	TLBP
Slug	1	199	0	0	0	99.5	ILBP
	1	195	2	1	1	97.5	TLBP
Bubble–slug	0	0	200	0	0	100	ILBP
	4	3	188	3	2	94	TLBP
Churn	0	1	0	199	0	99.5	ILBP
	1	4	2	184	9	92	TLBP
Slug–churn	0	1	0	0	199	99.5	ILBP
	2	3	4	6	185	92.5	TLBP

Table 2
Comparisons of classification accuracies of using BP neural network with ILBP and TLBP.

	Bubble	Slug	Bubble–slug	Churn	Slug–churn	Accuracies (%)	Method
Bubble	200	0	0	0	0	100	ILBP
	187	1	4	5	3	93.5	TLBP
Slug	0	199	0	0	1	99.5	ILBP
	2	188	2	3	5	94	TLBP
Bubble–slug	0	0	197	0	3	98.5	ILBP
	4	2	184	7	3	92	TLBP
Churn	0	0	0	200	0	100	ILBP
	3	5	4	177	11	88.5	TLBP
Slug–churn	0	1	1	0	198	99	ILBP
	2	3	3	9	183	91.5	TLBP

obtained was 95.39%. Obviously, our method achieves the best accuracy rate of 99.7% in average.

4.2. BP neural network

In this section, we use BP neural network to recognize the gas–liquid two-phase flow patterns for further validation. Zhou et al. (2005) and Sun et al. (2006) explored the similar work using neural networks, and obtained the classification accuracies of 93% and 91.5%, respectively.

In our experiments, we use the feed-forward BP neural network to train examples. By using the improved LBP operator, we obtain the recognition accuracy of 99.4%, which is better than the accuracy of 91.9% of using the traditional LBP operator. Table 2 shows the classification accuracies of the five flows using BP neural network with the improved LBP (denoted by ILBP) as compared with the traditional LBP (denoted by TLBP). From the table, we can see that the recognition accuracies of bubble–slug and slug–churn flows are a little bit lower than those of the other three flows. The result is consistent with the fact of the dynamic spatio-temporal movements of these lows.

5. Conclusions

Applying high-speed dynamic photography and digital image processing techniques to directly analyze flow patterns of evolving images explores a new approach to investigate the temporal and spatial evolution features of two-phase flow patterns. It is also a beneficial complement and reference for other indirect measurement used to analyze the structure and movement properties of flow patterns.

We have presented in this paper the improved LBP operator to recognize of gas–liquid two-phase flow patterns. We use the SVM and BP neural network tools to train and test the image features. Experimental results show that the improved LBP operator can describe the main characters of flow images more effectively than the traditional LBP operator. Furthermore, the method avoids complex calculation of feature extraction. In the future, we will focus on the pattern recognition by improved LBP operator under different neighborhoods and different radii.

Acknowledgements

This paper is supported by National Natural Science Foundation of China (ID: 50674070) and Post-Doctor Foundation of Ministry of Education of China (ID: 20070410757).

References

Ahonen, T., Hadid, A., Pietikainen, M., 2004. Face recognition with local binary patterns. In: Proceedings of European Conference on Computer Vision, Prague, Czech, pp. 469–481..
Bui, T., Dinh, Choi, T.S., 1999. Application of image processing techniques in air/water two phase flow. Mech. Res. Commun. 26, 463–468.
Chang, C.C., Lin, C.J., 2001. LIBSVM: A Library for Support Vector Machines [EB/OL]. <http://www.csie.ntu.edu.tw/~cjlin/papers/libsvm.pdf2001>.
Chang, C.C., Hsu, C.W., Lin, C.J., 2000. The analysis of decomposition methods for support vector machines. IEEE Trans. Neural Networks (11), 1003–1008.
Cortes, C., Vapnik, V.N., 1995. Support vector networks. Mach. Learn. 20, 273–297.
Gopal, M., Jepson, W.P., 1997. Development of digital image analysis techniques for the study of velocity and void profiles in slug flow. Int. J. Multiph. Flow 23, 945–965.
Hsieh, C.C., Wang, S.B., Pan, C., 1997. Dynamic visualization of two-phase flow patterns in a natural circulation loop. Int. J. Multiph. Flow 23, 1147–1170.
Lin, CJ., 2001. On the convergence of the decomposition method for support vector machines. IEEE Trans. Neural Networks 12, 1288–1298.
Maenpaa, T., 2003. The Local Binary Pattern approach to Texture Analysis Extensions and Applications. <http://herkules.oulu.fi/isbn9514270762/> (accessed 20.12.08).
Maenpaa, T., Pietikainen, M., 2003. Multi-scale binary patterns for texture analysis. In: Proceedings of the 13th Scandinavian Conference on Image Analysis, Goteborg, Sweden.
Maenpaa, T., Pietikainen, M., Ojala, T., 2000. Texture classification by multi-predicate local binary pattern operators. In: Proceedings of the 15th International Conference on Pattern Recognition, vol. 3. Barcelona, Spain, pp. 951–954.
Ojala, T., Pietikainen, M., Maenpaa, T., 2002. Multiresolution gray scale and rotation invariant texture analysis with local binary pattern. J. IEEE Trans. Pattern Anal. Mach. Intell. 24, 971–987.
Sathyamurthi, V., Banerjee, D., Sakamoto, H. et al., 2007. Measurement of the fractal order of wall void fractal during nucleate boiling. Int. J. Heat Fluid Flow.
Shi, L.L., Cai, H.J., Zhou, K.Z., 2005. Gas-liquid two-phase flow pattern identification base on image processing. J. Zhejiang Univ. (Eng. Sci.) 39, 1128–1131.
Sun, B., Wang, Q., Zhou, Y.L., 2006. Identification method of gas–liquid two-phase flow regime based on multi-scale information entropy feature and RBF neural network. Chinese J. Sci. Instrum. 27 (7), 725–729.
Vapnik, V.N., 1998. Statistical Learning Theory. Wiley, New York.
Zhang, W.Y., Jin, N.D., 2009. Improved local binary pattern based gas-liquid two-phase flow regimes analysis. In: The 6th International Conference on Fuzzy Systems and Knowledge Discovery, August 2009.
Zhao, X., Jin, N.D., Zhang, J.X., 2006. Flow pattern identification of gas/water two phase flow based on SVM. In: Proceedings of the 6th World Congress on Intelligent Control and Automation, vol. 6, pp. 56–61.
Zhou, Y.L., Sun, B., Lu, J., 2005. Application of improved BP neural network in identification of air–water two-phase flow patterns. J. Chem. Indus. Eng. 56, 110–115.
Zhou, Y.L., Li, H.W., Yuan, J.W., 2009. A new approach for identifying gas–liquid two-phase flow patterns. J. Eng. Therm. Energy Power 24, 68–72.